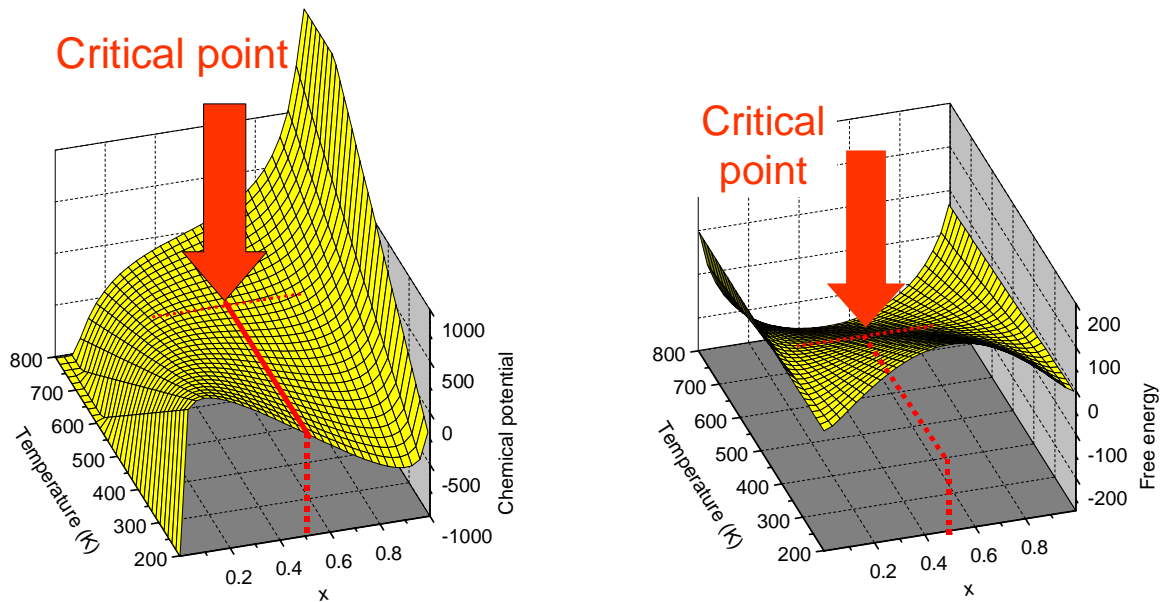


# IV CHAPTER : CRITICAL BEHAVIOUR, FLUCTUATIONS AND RANGE OF THE H-H INTERACTION

IV.1	Critical point behaviour.....	2
IV.2	Critical exponents of mean-field theories.....	6
IV.3	Validity of the Bragg-William approximation .....	11
IV.4	Influence of the interaction range on fluctuations .....	16
IV.5	Spinodal decomposition .....	19
IV.6	The elastic H-H interaction .....	25
IV.7	Lowering of $T_c$ in thin films .....	29
IV.8	Lowering of $T_c$ in amorphous materials .....	30

In this chapter we consider first the behaviour of a lattice-gas near the critical point and discuss the value of the so-called critical exponents within the mean-field theory and the Ising model. We show then that the existing experimental results imply that the H-H interaction must be long-ranged. Then we illustrate by means of Monte-Carlo simulations the role of the range of the interaction on fluctuations. Consequences of the long-range character of the H-H interaction (macroscopic density modes) are briefly discussed.



**Fig. IV.1:** Position of the critical point with respect to the isotherms of the chemical potential and the free energy of the lattice-gas, respectively.

## IV.1 CRITICAL POINT BEHAVIOUR

In this section we discuss the behaviour of the lattice-gas near the critical point (see Fig. IV.1) within the mean-field theory. As we shall see below, the critical point is determined by the conditions:

$$\frac{\partial \mu_H}{\partial c_H} = 0 \quad \text{and} \quad \frac{\partial^2 \mu_H}{\partial c_H^2} = 0 \quad (\text{IV.1})$$

It is well known that near the critical point the compressibility and the specific heat diverge like  $(T-T_c)^{-1}$ . The purpose of this paragraph is to investigate the behaviour of the lattice gas described by Eq.III.50 close to the critical point. The theoretical predictions shall be compared to experimental data for Pd<sup>1,2</sup> and for Pd<sub>0.9</sub>Ag<sub>0.1</sub> (Buck and Alefeld<sup>3</sup>).

To calculate the compressibility K of the lattice gas

$$K = -\frac{1}{V} \frac{\partial \mathcal{N}}{\partial p} \Big|_{T, N_H} \quad (\text{IV.2})$$

we start from Maxwell's relation (see Eq.III.7)

$$\frac{\partial \mu_H}{\partial p} \Big|_{T, N_H} = \frac{\partial \mathcal{N}}{\partial N_H} \Big|_{T, N_H} \quad (\text{IV.3})$$

Since  $\mu_H$  depends only on the intensive variables p, T and  $c_H$  we have

$$\frac{\partial \mu_H}{\partial p} \Big|_{T, N_H} = \frac{\partial \mu_H}{\partial c_H} \Big|_{p, T} \frac{\partial c_H}{\partial p} \Big|_{T, N_H} \quad (\text{IV.4})$$

The pressure dependence of  $\mu_H$  is neglected because  $\epsilon_0$  and  $\epsilon$  in Eq.III.52 are treated as constants. For the evaluation of the partial derivatives in Eq.IV.xx we introduce the density of H atoms per volume

$$\rho = \frac{N_H}{V} = c_H \frac{N}{V} \equiv c_H \rho_{mi} \quad (\text{IV.5})$$

The density of interstitial sites  $\rho_{mi} = N/V$  is a constant that depends only on the host lattice. Then

$$\frac{\partial \mathcal{N}}{\partial N_H} \Big|_{p, T} = \frac{1}{\rho_{mi} c_H} \quad (\text{IV.6})$$

and

$$\left. \frac{\partial c_H}{\partial p} \right|_{T, N_H} = \frac{1}{\rho_{mi}} \left. \frac{\partial \left( \frac{N_H}{V} \right)}{\partial p} \right|_{T, N_H} = \frac{1}{\rho_{mi}} \left( \frac{N_H}{V^2} \frac{\partial V}{\partial p} \right) \Big|_{T, N_H} = c_H K \quad (\text{IV.7})$$

Finally

$$\frac{1}{K} = \rho_{mi} c_H^2 \left. \frac{\partial \mu_H}{\partial c_H} \right|_T \quad (\text{IV.8})$$

According to Eq.IV.6 the compressibility is thus directly related to the concentration dependence of the chemical potential  $\mu_H$ . The quantity  $(\partial \mu_H / \partial c_H)_T$  is related to the pressure of the  $H_2$ -gas surrounding the sample through  $\mu_H = 1/2 \mu_{H_2}$  which leads to

$$\frac{\partial \mu_H}{\partial c_H} = \frac{1}{2} kT \frac{1}{p_{H_2}} \frac{dp_{H_2}}{dc_H} \quad (\text{IV.9})$$

and is thus accessible to the experiment. From Eq.IV.6 we obtain

$$\frac{1}{K} = \rho_{mi} c_H^2 \left[ kT \frac{1}{c_H(1-c_H)} + \varepsilon n \right] \quad (\text{IV.10})$$

and from Eq.III.76

$$\frac{1}{K} = \rho_{mi} c_H^2 k \left[ \frac{T}{c_H(1-c_H)} - 4T_c \right] \quad (\text{IV.11})$$

On a line of constant concentration  $c_H = c_{\text{critical}} = 1/2$ , the compressibility diverges according to

$$K = \frac{1}{\rho_{mi} k} \frac{1}{T - T_c} \quad (\text{IV.12})$$

In the theory of critical phenomena it is usual to define so-called **critical exponents**. The critical exponent corresponding to  $K$  is designated by  $\gamma$  and defined by

$$K = \text{const.} (T - T_c)^{-\gamma} \quad (\text{IV.13})$$

A comparison of Eq.IV.12 and Eq.IV.13 shows that

$$\gamma = 1 \quad (IV.14)$$

This value is in excellent agreement with the experimental values for  $\text{Pd}_{0.9}\text{Ag}_{0.1}\text{H}_x$  and  $\text{PdH}_x$  (see Table IV.1).

Another critical exponent ( $\beta$ ) is defined by the shape of the coexistence curve in the vicinity of the critical point by the relation

$$-(T - T_c) = \text{const.} \cdot (c - c_{\text{critical}})^{1/\beta} \quad (IV.15)$$

In our model,  $\beta$  may be determined from a series expansion around  $c_{\text{critical}}$  of Eq.III.69 writing  $c - c_c = \delta$  we obtain with  $c_c = 1/2$

$$kT \ln \frac{\delta + 1/2}{1/2 - \delta} + \epsilon n \delta = 0 \quad (IV.16)$$

with

$$\ln \frac{1 + 2\delta}{1 - 2\delta} = 2 \left[ 2\delta + \frac{8\delta^3}{3} + \dots \right] \quad (IV.17)$$

and, finally,

$$-\left( \frac{T - T_c}{T_c} \right) = \frac{4}{3} (c - c_c)^2 \quad (IV.18)$$

Which means that here

$$\beta = 1/2 \quad (IV.19)$$

This value is also in good agreement with the data of De Ribaupierre and Manchester as can be seen from Table IV.1.

We shall now comment on the data indicated in Table IV.1. First we have to define the names **mean field theory** and **3-dim Ising model**.

The theory which is presented above is based on the Bragg-William approximation which assumes that the H-H interaction can be evaluated from the average (mean-field) distribution of hydrogen atoms in the lattice. This theory is similar to that of the mean-magnetic-field theory of ferromagnets and antiferromagnets (see for example Ashcroft and Mermin<sup>4</sup> page 715-418).

The 3-dimensional Ising model is a model for a magnetic substance for which the magnetic moments are distributed on a regular lattice and can have only two values, spin-up or spin-down. As shown by Lee and Yang<sup>5</sup> the 3-dimensional Ising model is also a model for binary alloys and for lattice gases. In Table IV.1, 3-dim Ising model means that the critical exponents have been

calculated from Eq.III.43 without approximations. Until now, nobody has succeeded in solving analytically the 3-dim Ising model and the values in Table IV.1, are evaluated from computer calculations.

**Table IV.1:** Experimental and theoretical values for the critical exponent  $\beta$  (coexistence line) and  $\gamma$  (compressibility) for various systems.

System	$\beta$		$\gamma$	
	Experiment	Mean field theory	Experiment	Mean field theory
CO <sub>2</sub>	0.35	1/2	1.26	1
Xe	0.35		1.26	
<sup>4</sup> He	0.359		1.24	
<sup>3</sup> He	0.361		1.18	
O <sub>2</sub>	0.353		1.25	
n-pentane	0.35		1.25	
CrBr <sub>3</sub>	0.368		1.21	
Gd	0.37	1/2	1.25	1
Ni	0.37		1.28	
YIG $\equiv$ Y <sub>3</sub> Fe <sub>5</sub> O <sub>12</sub>	0.38		1.31	
Pd-H <sup>(a)</sup>	0.55	1/2	1.01 $\pm$ 0.1	1
Pd <sub>0.9</sub> Ag <sub>0.1</sub> H <sup>(b)</sup>			1.02 $\pm$ 0.04	
EuO	0.368		1.29	

a) From de Ribaupierre and Manchester (refs.1, 2)

b) Buck and Alefeld (ref. 3)

\*)Table in part out Capocaccia et al.<sup>6</sup> and Stanley<sup>7</sup>

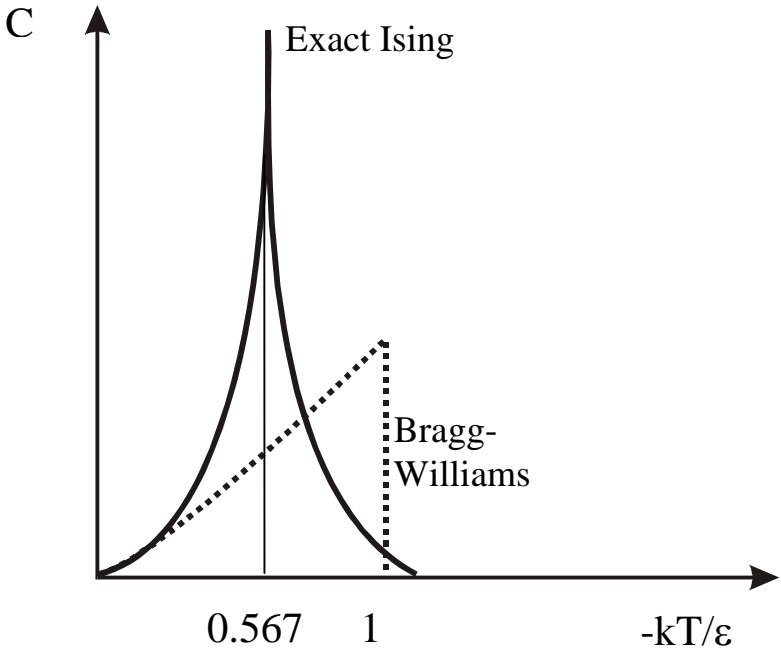


**Fig. IV.2:** The specific heat of a square lattice gas. The exact solution is due to Onsager. Near  $T_c$  it diverges while the Bragg-William approximation has a jump.

For a 2-dim system, however, Onsager<sup>8</sup> did find an analytical solution. It is rather instructive to compare the exact solution for the specific heat of a lattice gas to the prediction of the Bragg-William (mean-field) theory. Fig. IV.2 shows clearly how different both solutions are. The exact solution has a log-singularity at the critical point and is symmetric (approximately) while the Bragg-William theory predicts a jump at  $T=T_c$  and does not diverge at the critical point.

We have thus the very curious situation in metal-hydrides that they are *better* described by the *approximate* mean-field theory than by the *exact* theory ! Among all the other examples mentioned in Table IV.1, the hydrides are thus the only substance which can be described by the mean field theory.

There are two important questions to ask here:

- 1) Does the good agreement between experimental and theoretical critical exponents for hydrides prove that the Bragg-William approximation is good ?
- 2) When is the Bragg-William approximation good for the exact problem defined by Eq.III.43 ?

## IV.2 CRITICAL EXPONENTS OF MEAN-FIELD THEORIES

The answer to the first question is quite disappointing, as we are going to show that if the thermodynamical potentials do not have mathematical singularities, the critical exponents are the same for every model. For this, let us consider the case of  $N_H$  H-atoms “dissolved” in  $N$  interstitial sites. The change  $\delta U$  in the internal energy of the system at  $p=p_0$  and  $T=T_0$  is

$$\delta U = \delta Q^\downarrow - p_0 \delta V + \mu_H \delta N_H \quad (\text{IV.20})$$

From the second law of thermodynamics

$$\delta S \geq \frac{\delta Q^\downarrow}{T_0} \quad (\text{IV.21})$$

and thus

$$T_0 \delta S \geq \delta U + p_0 \delta V - \mu_H \delta N_H \quad (\text{IV.22})$$

and

$$\delta U + p_0 \delta V - T_0 \delta S - \mu_H \delta N_H \leq 0 \quad (\text{IV.23})$$

Thus in any naturally occurring process the quantity on the left side of Eq.IV.23 decreases and eventually reaches a minimum at equilibrium. This means that for little virtual excursions of the system

$$\delta U + p_0 \delta V - T_0 \delta S - \mu_H \delta N_H \geq 0 \quad (\text{IV.24})$$

We assume now that  $\delta U$  can be developed in a series (no singularity of U). Thus

$$\begin{aligned} \delta U &= \frac{\partial U}{\partial S} \delta S + \frac{\partial U}{\partial V} \delta V + \frac{\partial U}{\partial N_H} \delta N_H \\ &+ \frac{1}{2} \left[ \frac{\partial^2 U}{\partial S^2} \delta S^2 + \frac{\partial^2 U}{\partial V^2} \delta V^2 + \frac{\partial^2 U}{\partial N_H^2} \delta N_H^2 \right. \\ &\left. + 2 \frac{\partial^2 U}{\partial S \partial V} \delta S \delta V + 2 \frac{\partial^2 U}{\partial V \partial N_H} \delta V \delta N_H + 2 \frac{\partial^2 U}{\partial S \partial N_H} \delta S \delta N_H \right] \end{aligned} \quad (\text{IV.25})$$

Inserting Eq.IV.25 in Eq.IV.24 and realizing that

$$\frac{\partial U}{\partial S} = T_0, \quad \frac{\partial U}{\partial V} = -p_0 \quad \text{and} \quad \frac{\partial U}{\partial N_H} = \mu_H \quad (\text{IV.26})$$

we obtain that the term within brackets [...]  $\geq 0$ . This implies that the following conditions must be satisfied

$$\frac{\partial^2 U}{\partial S^2} \geq 0 \quad (\text{IV.27})$$

$$\begin{vmatrix} \frac{\partial^2 U}{\partial S^2} & \frac{\partial^2 U}{\partial S \partial V} \\ \frac{\partial^2 U}{\partial V \partial S} & \frac{\partial^2 U}{\partial V^2} \end{vmatrix} \geq 0 \quad (\text{IV.28})$$

$$\begin{vmatrix} \frac{\partial^2 U}{\partial S^2} & \frac{\partial^2 U}{\partial S \partial V} & \frac{\partial^2 U}{\partial S \partial N_H} \\ \frac{\partial^2 U}{\partial V \partial S} & \frac{\partial^2 U}{\partial V^2} & \frac{\partial^2 U}{\partial V \partial N_H} \\ \frac{\partial^2 U}{\partial N_H \partial S} & \frac{\partial^2 U}{\partial N_H \partial V} & \frac{\partial^2 U}{\partial N_H^2} \end{vmatrix} \geq 0 \quad (\text{IV.29})$$

which can be rewritten as follows by using Eq.IV.26 but dropping the index  $_0$  for  $T_0$  and  $p_0$

$$\frac{\partial T}{\partial S} \geq 0 \quad (\text{IV.30})$$

$$\begin{vmatrix} \frac{\partial T}{\partial S} & -\frac{\partial p}{\partial S} \\ \frac{\partial T}{\partial V} & -\frac{\partial p}{\partial V} \end{vmatrix} \geq 0 \quad (\text{IV.31})$$

$$\begin{vmatrix} \frac{\partial T}{\partial S} & -\frac{\partial p}{\partial S} & \frac{\partial \mu_H}{\partial S} \\ \frac{\partial T}{\partial V} & -\frac{\partial p}{\partial V} & \frac{\partial \mu_H}{\partial V} \\ \frac{\partial \mathcal{N}}{\partial T} & \frac{\partial \mathcal{N}}{\partial p} & \frac{\partial \mathcal{N}}{\partial \mu_H} \\ \frac{\partial \mathcal{N}_H}{\partial T} & \frac{\partial \mathcal{N}_H}{\partial p} & \frac{\partial \mathcal{N}_H}{\partial \mu_H} \end{vmatrix} \geq 0 \quad (\text{IV.32})$$

Multiplying the two determinants by -1 and using the functional determinant notation defined as follows

$$\frac{\partial(y_1, \dots, y_n)}{\partial(x_1, \dots, x_n)} = \begin{vmatrix} \frac{\partial y_1}{\partial x_1} & \dots & \frac{\partial y_n}{\partial x_1} \\ \vdots & \ddots & \vdots \\ \frac{\partial y_1}{\partial x_n} & \dots & \frac{\partial y_n}{\partial x_n} \end{vmatrix} \quad (\text{IV.33})$$

we may write

$$\frac{\partial(T, V, N_H)}{\partial(S, V, N_H)} \geq 0 \quad \frac{\partial(T, p, N_H)}{\partial(S, V, N_H)} \leq 0 \quad \frac{\partial(T, p, \mu_H)}{\partial(S, V, N_H)} \leq 0 \quad (\text{IV.34})$$

Dividing the first condition by the second we have

$$\frac{\partial(T, V, N_H)}{\partial(T, p, N_H)} \leq 0 \quad \rightarrow \quad \left. \frac{\partial \mathcal{N}}{\partial p} \right|_{T, N_H} \leq 0 \quad (\text{IV.35})$$

Dividing the third condition by the second we have

$$\frac{\partial(T, p, \mu_H)}{\partial(T, p, N_H)} \geq 0 \quad \rightarrow \quad \left. \frac{\partial \mu_H}{\partial N_H} \right|_{p, T} = \frac{1}{N} \left. \frac{\partial \mu_H}{\partial c_H} \right|_{p, T} \geq 0 \quad (\text{IV.36})$$

The first condition implies also that

$$C_v \geq 0 \quad (\text{IV.37})$$

All three conditions must be satisfied by our lattice gas model. We used previously the condition  $\partial \mu_H / \partial c_H \geq 0$  to show that some part of the solubility isotherm was unphysical.

This discussion of thermodynamical inequalities is of course only correct if the second order term  $1/2[\dots]$  in Eq.IV.25 does not vanish identically, because if  $[\dots]=0$  then higher order terms must be included. Let us investigate what happens when the second order term vanishes. For this we rewrite Eq.IV.25 as

$$\begin{aligned} \delta U - T\delta S + p\delta V + \mu_H \delta N_H &= \\ \frac{1}{2} \left[ \delta \left( \frac{\partial U}{\partial S} \right) \delta S + \delta \left( \frac{\partial U}{\partial V} \right) \delta V + \delta \left( \frac{\partial U}{\partial N_H} \right) \delta N_H \right] & \quad (\text{IV.38}) \\ = \frac{1}{2} [\delta T \delta S + (-\delta p) \delta V + \delta \mu_H \delta N_H] & \end{aligned}$$

We have also

$$\delta \mu_H = \frac{\partial \mu_H}{\partial p} \delta p + \frac{\partial \mu_H}{\partial T} \delta T + \frac{\partial \mu_H}{\partial N_H} \delta N_H \quad (\text{IV.39})$$

One sees thus that the second order term  $1/2[\dots]$  in Eq.IV.25 vanishes identically if  $\delta p=0$ ,  $\delta T=0$  and

$$\left. \frac{\partial \mu_H}{\partial N_H} \right|_{p,T} = 0 \quad (\text{IV.40})$$

From the definition of the **spinodal curve** (see Eq.III.87) we see that the points where  $1/2[\dots]=0$  must lie on the spinodal.

We shall now show that the condition Eq.IV.24 for thermodynamical equilibrium implies further conditions for  $\mu_H$ .

At constant pressure and temperature Eq.IV.24 can be written as

$$\delta G - \mu_H \delta N_H \geq 0 \quad (\text{IV.41})$$

because of  $G=U-TS+pV$ . For  $\delta p=0$  and  $\delta T=0$  we may write

$$\begin{aligned} \delta G &= \frac{\partial G}{\partial N_H} \delta N_H + \frac{1}{2} \frac{\partial^2 G}{\partial N_H^2} \delta N_H^2 + \frac{1}{6} \frac{\partial^3 G}{\partial N_H^3} \delta N_H^3 \\ &+ \frac{1}{24} \frac{\partial^4 G}{\partial N_H^4} \delta N_H^4 + \dots \end{aligned} \quad (\text{IV.42})$$

The condition Eq.IV.41 becomes then with  $\partial G/\partial N_H=\mu_H$

$$\frac{1}{2} \frac{\partial^2 G}{\partial N_H^2} \delta N_H^2 + \frac{1}{6} \frac{\partial^3 G}{\partial N_H^3} \delta N_H^3 + \frac{1}{24} \frac{\partial^4 G}{\partial N_H^4} \delta N_H^4 + \dots \geq 0 \quad (\text{IV.43})$$

$$\frac{\partial \mu_H}{\partial N_H} \delta N_H^2 + \frac{1}{3} \frac{\partial^2 \mu_H}{\partial N_H^2} \delta N_H^3 + \frac{1}{12} \frac{\partial^3 \mu_H}{\partial N_H^3} \delta N_H^4 + \dots \geq 0 \quad (\text{IV.44})$$

On the spinodal  $\partial \mu / \partial N_H = 0$  and thus

$$\frac{\partial^2 \mu_H}{\partial N_H^2} \delta N_H^3 + \frac{1}{4} \frac{\partial^3 \mu_H}{\partial N_H^3} \delta N_H^4 \geq 0 \quad (\text{IV.45})$$

This implies that

$$\left. \frac{\partial^2 \mu_H}{\partial N_H^2} \right|_{p,T} = 0 \quad (\text{IV.46})$$

and

$$\left. \frac{\partial^3 \mu_H}{\partial N_H^3} \right|_{p,T} > 0 \quad (\text{IV.47})$$

The two conditions  $\frac{\partial \mu_H}{\partial N_H} = 0$  and  $\frac{\partial^2 \mu_H}{\partial N_H^2} = 0$  define the critical pressure and temperature of the critical point. In the vicinity of the critical point we can write

$$\begin{aligned} \frac{\partial \mu_H}{\partial c_H}(c_H, T) &= \underbrace{\frac{\partial \mu_H}{\partial c_H}(c_c, T_c)}_{=0} + \frac{\partial^2 \mu_H}{\partial T \partial c_H} (T - T_c) \\ &+ \underbrace{\frac{\partial^2 \mu_H}{\partial c_H^2}(c_H - c_c)}_{=0} + \frac{1}{2} \frac{\partial^3 \mu_H}{\partial c_H^3} (c_H - c_c)^2 + \dots \end{aligned} \quad (\text{IV.48})$$

By integration at  $T = \text{const.}$

$$\mu_H(c_H, T) - \mu_H(c_c, T_c) = A(T - T_c)(c_H - c_c) + B(c_H - c_c)^3 \quad (\text{IV.49})$$

and from Eq.IV.6

$$K = \frac{1}{\rho_{mi} c_H} \frac{1}{\frac{\partial \mu}{\partial c_H}} = \frac{1}{\rho_{mi} c_c^2 A (T - T_c)} \quad (\text{IV.50})$$

and thus  $\gamma = 1$ . Similarly, the shape of the spinodal is obtained from Eq.IV.48 by setting  $\partial \mu_H / \partial c_H = 0$  (definition of the spinodal)

$$0 = A(T - T_c) + (-3B)(c_H - c_c)^2 \quad (\text{IV.51})$$

which is exactly the same form as Eq.IV.18 and

$$\beta = \frac{1}{2} \quad (\text{IV.52})$$

We arrive thus at the conclusion that critical exponents do not depend on a particular model for the substance under consideration as long as the thermodynamic quantities U, F, etc. are regular functions. We conclude furthermore that the experimental results obtained for PdH<sub>x</sub> and Pd<sub>0.9</sub>Ag<sub>0.1</sub>H<sub>x</sub> (see Table IV.1) show that the thermodynamical functions of these hydrides are regular functions at the critical point. Note, however, that this conclusion is only valid if one believes that the experiments done on these hydrides were done close enough to the critical point. This brings us to the second question mentioned above

### IV.3 VALIDITY OF THE BRAGG-WILLIAM APPROXIMATION

In the Bragg-William approximation we have assumed that the distribution of hydrogen's in a metal was well described by the *average density* of hydrogen's in the metal. In other words one expects the Bragg-William approximation to be good if the fluctuation of the number of hydrogen's in a certain volume is small; more precisely when the fluctuation in the interaction energy of a given H-atom with all other hydrogen's is small. Let us assume here that the range of the H-H pair interaction is b (this is a generalisation of the model given by Eq.III.42 where only nearest neighbour interaction was taken into account). The fluctuation in the interaction energy is then approximately proportional to the fluctuation  $\Delta n_H$  of the  $n_H$  hydrogen "atoms" contained in a sphere of radius b.

$$n_H = \frac{4\pi b^3}{3} \frac{N_H}{N} \frac{N}{V} = \frac{4\pi b^3}{3} c_H \rho_{mi} \quad (\text{IV.53})$$

For a FCC metal in which H is occupying octahedral sites (e.g. PdH<sub>x</sub>),  $\rho_{mi}=4/a^3$  where  $a$  is the lattice constant of the host metal. At the critical concentration we have thus ( $c_c=1/2$ )

$$n_H = \frac{8\pi}{3} \left(\frac{b}{a}\right)^3 \quad (\text{IV.54})$$

To evaluate the fluctuation in  $n_H$  let us proceed as follows. The equation of Boltzmann

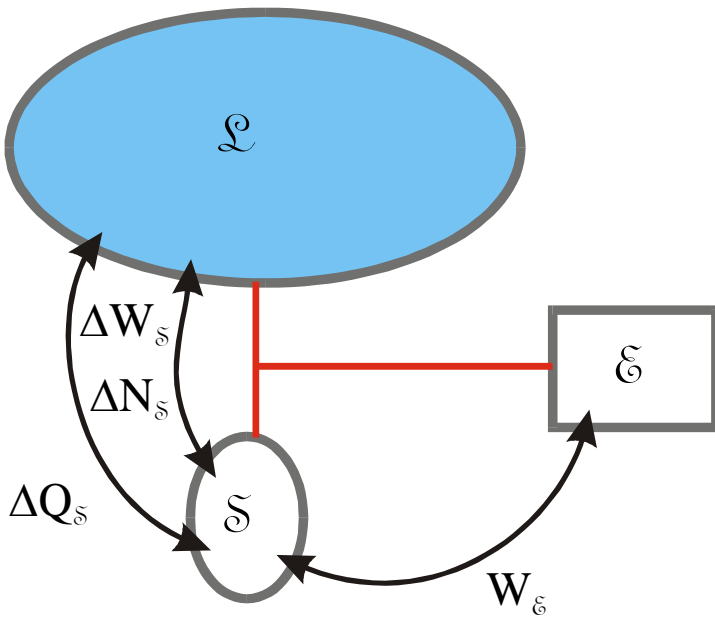
$$S = k \ln \omega \quad (\text{IV.55})$$

relates the entropy of a system to the number of microstates  $\omega$  of given total energy. This suggests that the probability of a fluctuation is proportional to  $e^S$  or  $e^{\Delta S/k}$  with  $\Delta S=S-S_0$  ( $S$  is the entropy of a closed system with a given fluctuation and  $S_0$  is the value of the entropy at equilibrium). To calculate  $\Delta S$  let us consider a situation in which a large system  $\mathcal{L}$  (which determines the equilibrium pressure  $p_L=p_0$  and temperature  $T_L=T_0$ ) contains a small system  $\mathcal{S}$  which can be brought out of equilibrium by a source  $\mathcal{E}$  (see Fig. IV.3).

The total entropy  $S_0$  is, at equilibrium

$$S_0 = S_{L_0} + S_{S_0} + S_{E_0} \tag{IV.56}$$

Let us assume that at first  $\mathcal{E}$  is not connected with  $\mathcal{S}$  and  $\mathcal{L}$  but that  $\mathcal{S}$  and  $\mathcal{L}$  can exchange heat, particles and work. If a fluctuation brings the small system  $\mathcal{S}$  out of equilibrium with the large system  $\mathcal{L}$  then the total entropy must decrease ( $S_0$  is the maximum value of  $S$  for a closed system of constant internal energy  $U_0$ ). Graphically we have the situation shown in Fig. IV.4. This graph shows immediately that the same fluctuation could be realised in doing some work on the  $\{\mathcal{L}+\mathcal{S}\}$  system at constant entropy  $S$ . This is the reason why we chose an insulated work source in Fig. IV.3



$$S_0 - S = \frac{\partial S}{\partial U}(U_0 - U) = \frac{W_E}{T_0}$$

$$\Delta S = -\frac{W_E}{T_0}$$

**Fig. IV.3:** Situation considered to calculate fluctuations. The entire system is treated as a closed system.

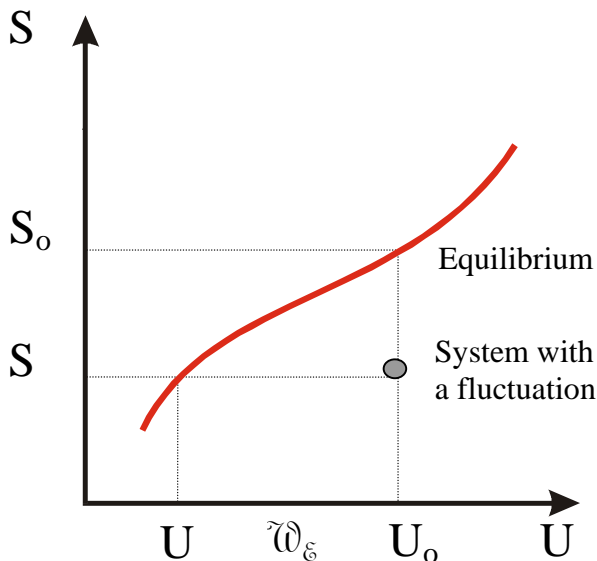


**Fig. IV.4:** A change in entropy arising from a fluctuation can also be realised by doing some work on the  $\mathcal{L}+\mathcal{S}$  system in Fig. IV.3.

The probability of having a certain fluctuation is thus given by

$$\omega \sim e^{-W_E/kT_0} \quad (\text{IV.58})$$

where  $W_E$  is the work done by the source  $\mathfrak{E}$  on  $\mathfrak{S}$  to bring it out of equilibrium with  $\mathfrak{L}$ . From the first law of thermodynamics we have, however

$$\Delta U_S = -T_0 \Delta S_L + p_0 \Delta V_L + \mu \Delta N_S + W_E \quad (\text{IV.59})$$

The total system  $\{\mathfrak{L} + \mathfrak{S} + \mathfrak{E}\}$  being closed we have that

$$\Delta S_L + \Delta S_S + \Delta S_E = 0 \quad (\text{IV.60})$$

The source  $\mathfrak{E}$  being thermally insulated we have further  $\Delta S_E = 0$  and thus

$$\Delta S_L = -\Delta S_S \quad (\text{IV.61})$$

Another implication of the assumption of a closed system is that  $\Delta V = \Delta V_S + \Delta V_L = 0$ . Thus finally

$$\Delta U_S = T_0 \Delta S_S - p_0 \Delta V_S + \mu \Delta N_S + W_E \quad (\text{IV.62})$$

$$W_E = \Delta(U_S - T_0 S_S + p_0 V_S) - \mu \Delta N_S \quad (\text{IV.63})$$

$$W_E = \Delta G - \mu \Delta N_S \quad (\text{IV.64})$$

Thus at  $p$  and  $T$  constant and with the notation used for metal-hydrides

$$\omega \sim e^{-(\Delta G - \mu_H \Delta n_H)/kT} \quad (\text{IV.65})$$

Writing

$$\Delta G = \frac{\partial G}{\partial n_H} \Delta n_H + \frac{1}{2} \frac{\partial^2 G}{\partial n_H^2} (\Delta n_H)^2 + \dots = \mu_H \Delta n_H + \frac{1}{2} \frac{\partial^2 G}{\partial n_H^2} (\Delta n_H)^2 \quad (\text{IV.66})$$

we obtain

$$\omega_{n_H} \sim \exp \left[ \frac{-\frac{1}{2} \left( \frac{\partial \mu_H}{\partial n_H} \right) (\Delta n_H)^2}{kT} \right] \quad (\text{IV.67})$$

This is a Gaussian curve centred at  $n_H$ . For a normalised Gaussian curve

$$w(x) = \sqrt{\frac{\beta}{2\pi}} e^{-\frac{\beta}{2} x^2} \quad (\text{IV.68})$$

and the integral

$$\int_{-\infty}^{\infty} x^2 e^{-\frac{\beta}{2} x^2} dx = \sqrt{\frac{2}{\beta}} \quad (\text{IV.69})$$

is equal to  $1/\beta$ . The mean value of  $(\Delta n_H)^2$  is thus

$$(\Delta n_H)^2 = \frac{kT}{\left( \frac{\partial \mu_H}{\partial n_H} \right)_{p,T}} \quad (\text{IV.70})$$

According to what was said above one expects the Bragg-William approximation to be valid if

$$\frac{(\Delta n_H)^2}{(n_H)^2} \ll 1 \quad (\text{IV.71})$$

which implies (with  $V_b = 4\pi b^3/3$ ) that

$$\frac{kT}{\bar{n}_H^2 \left( \frac{\partial \mu_H}{\partial n_H} \right)_{p,T}} = \frac{kT}{c_H^2 \rho_{mi}^2 V_b^2 \frac{1}{\rho_{mi} V_b} \frac{\partial \mu_H}{\partial c_H}} = \frac{kT}{c_H^2 \rho_{mi} V_b \frac{\partial \mu_H}{\partial c_H}} \ll 1 \quad (\text{IV.72})$$

Close to the critical point (see Eq.IV.48)

$$\frac{kT_c}{c_H^2 \rho_{mi} V_b A(T - T_c)} \ll 1 \quad (\text{IV.73})$$

For the case of PdH<sub>x</sub>,  $\rho_{\text{mi}}V_b=(16\pi/3)(b/a)^3$  and in the Bragg-William approximation  $c_H=1/2$  and  $A=(\partial^2\mu_H/\partial T\partial c_H)_{cc,T_c}=4k$  so that Eq.IV.73 becomes

$$\frac{T-T_c}{T_c} \gg \frac{3}{16\pi} \left(\frac{a}{b}\right)^3 \quad (\text{IV.74})$$

Both in PdH<sub>x</sub> (de Ribaupierre and Manchester) and in Pd<sub>0.9</sub>Ag<sub>0.1</sub>H<sub>x</sub> (Buck and Alefeld) the mean-field theory has been found to be valid for  $(T-T_c)/T_c > 10^{-3}$ . From Eq.IV.74 we have then

$$10^{-1} \sqrt[3]{\frac{16\pi}{3}} \gg \frac{a}{b} \rightarrow b \gg 3a \quad (\text{IV.75})$$

This suggests that the interaction between two hydrogen's in a metal is a long range interaction with  $b \sim 100-1000 \text{ \AA}$  ( $a \cong 4 \text{ \AA}$  for most transition metals). Summarising, we know now that the H-H in a metal is

- attractive ( $\varepsilon < 0$ ) (IV.76)

- of the order of a few hundredths of eV (IV.77)

- long-ranged, such that  $\varepsilon(r) \sim \frac{1}{r^{3+\lambda}}$  with  $\lambda > 0$  (IV.78)

The property (Eq.IV.77) follows from the fact that if the interaction energy is written as a function of the distance between two hydrogen's, the total interaction energy

$$\int \varepsilon(r) \frac{4\pi r^2}{a^3} dr = E_{\text{int}} < \infty \quad (\text{IV.79})$$

must remain finite. In a later chapter we shall show that the elastic interaction between two hydrogen's imbedded in a deformable host lattice satisfies the conditions 1 to 4.

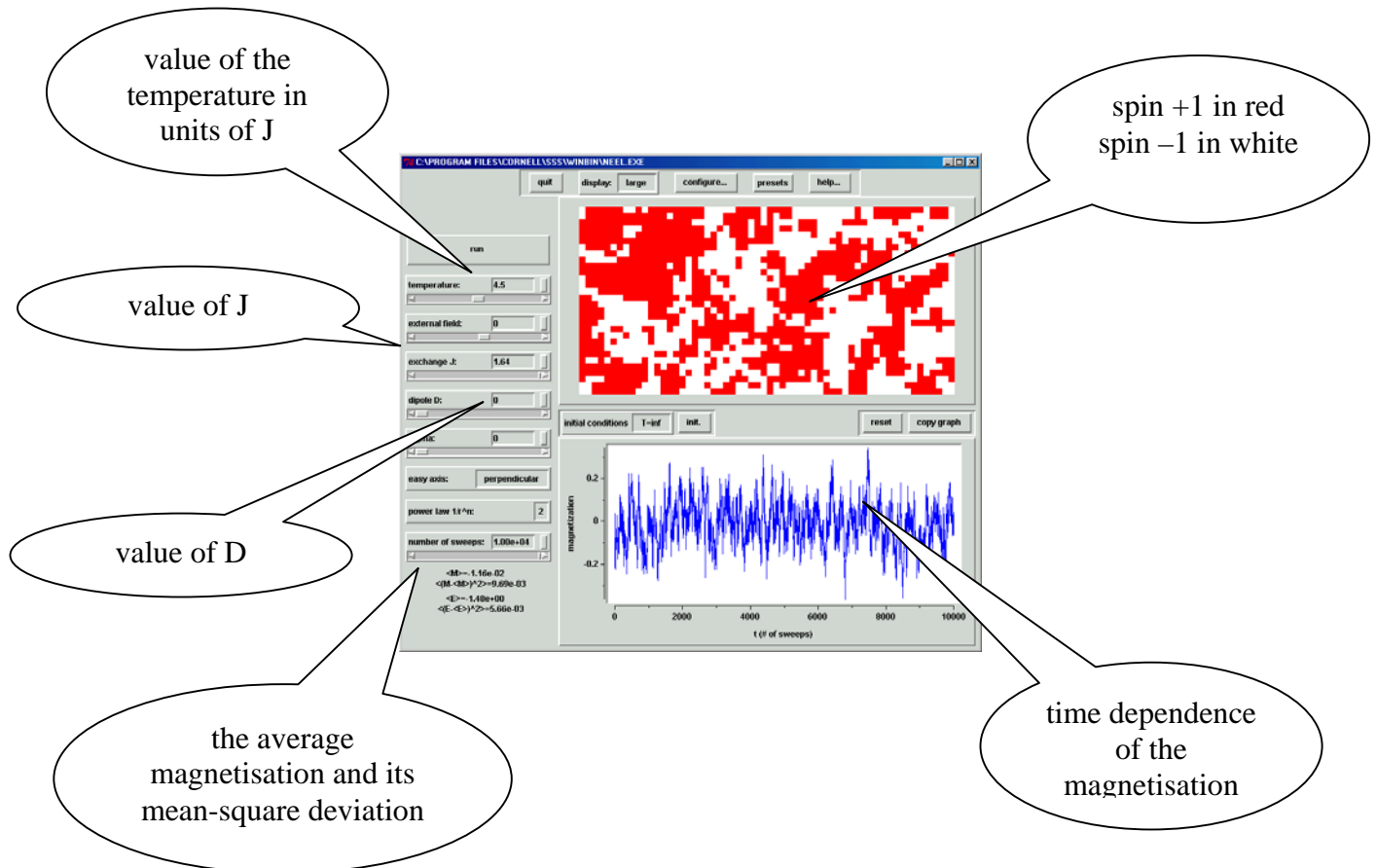
In Section IV.4 we investigate the role of the interaction range on fluctuations quantitatively by means of a two-dimensional Monte-carlo simulation. After that, we will continue with the H-H interaction in metal-hydrogen systems.

## IV.4 INFLUENCE OF THE INTERACTION RANGE ON FLUCTUATIONS

One expects that fluctuations are suppressed when the interaction range is increasing. This can be nicely demonstrated by using the Monte-Carlo program called Neel. This program calculates the total energy of a so-called Ising model (see Eq.IV.80) for a collection of  $N$  atoms distributed on a  $N_x \times N_y$  square lattice, with spin variables that can take only the values  $+1$  and  $-1$ . The spins are assumed to interact with their nearest neighbours through an exchange interaction  $-J$  if the neighbour is parallel and  $+J$  if the neighbour is antiparallel. The exchange interaction is zero for more distant neighbours. This means that the first sum in Eq. IV.80 is taken only over all the pairs of nearest neighbours. The factor  $\frac{1}{2}$  takes care of the double counting of the interactions. A positive  $J$  favours a parallel alignment of spins (ferromagnetic order) while a negative  $J$  leads to antiferromagnetic ordering. In addition the model incorporates a dipolar term between all spins with a strength  $D$  and a  $1/r^2$ –dependence. A positive  $D$  favours the antiparallel alignment of spins. This model can be mapped onto the lattice gas model by taking spin  $+1$  as an occupied interstitial and  $-1$  as an empty site. Then  $J$  is a measure of a hypothetical short range H-H interaction and  $D$  is a measure of a hypothetical long-range H-H interaction.

$$H = -\frac{J}{2} \sum \mathbf{S}_i \mathbf{S}_j + \frac{D}{2} \sum \frac{a^2}{R_{ij}^2} \mathbf{S}_i \mathbf{S}_j \quad (\text{IV.80})$$

The output of the program consists of:



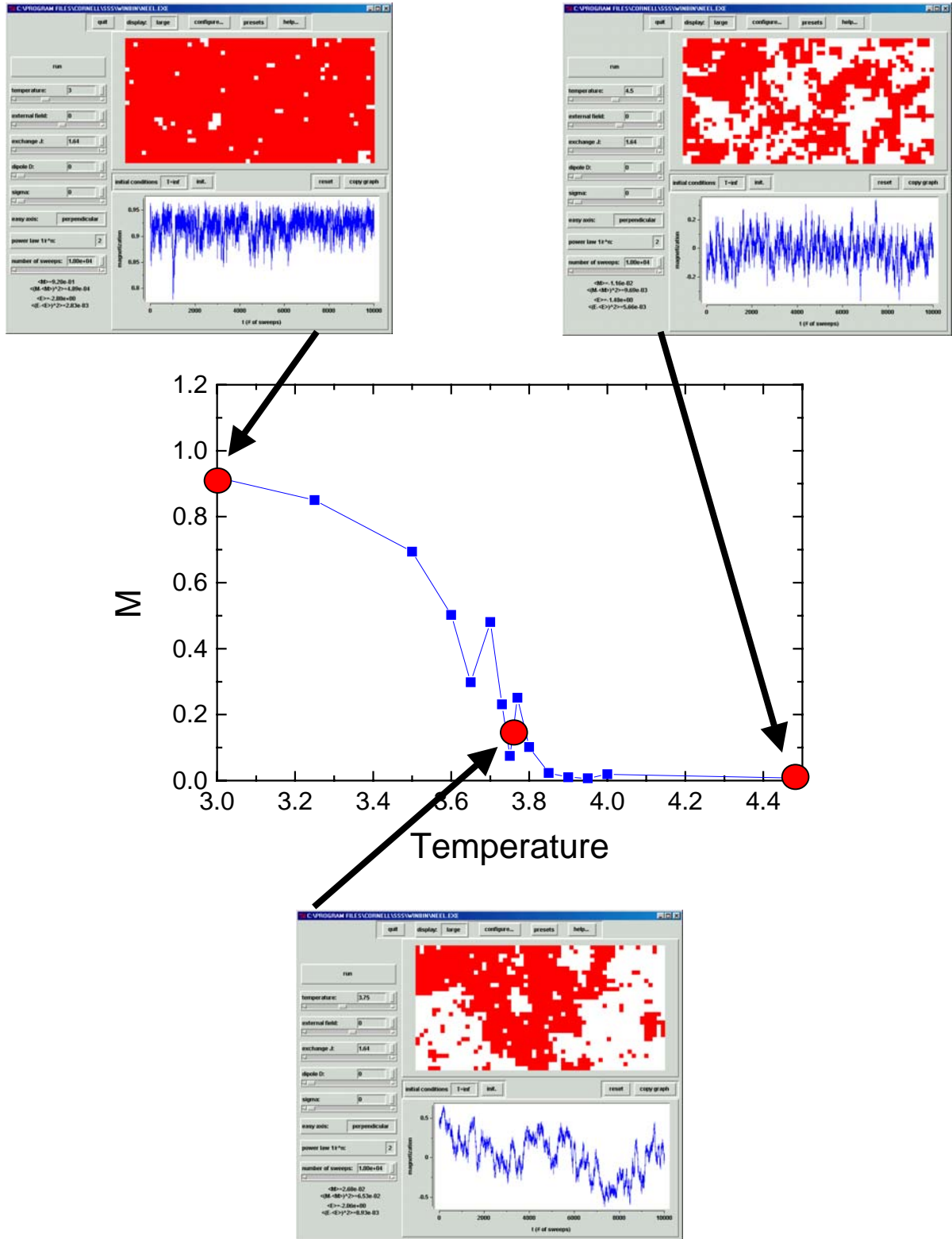


**Fig. IV.5:** Results of a Monte-Carlo simulation for  $J=1.64$  at three temperatures:  $T=3$  J,  $3.75$  J and  $4.5$  J in the absence of dipolar interaction. The magnetisation is normalised to 1. Large fluctuations occur close to  $T=3.75$ . From the lower panel we conclude that the magnetisation can even reverse sign as a function of time. The spiky structure near  $T=3.75$  J arise from the finite time of the simulations.

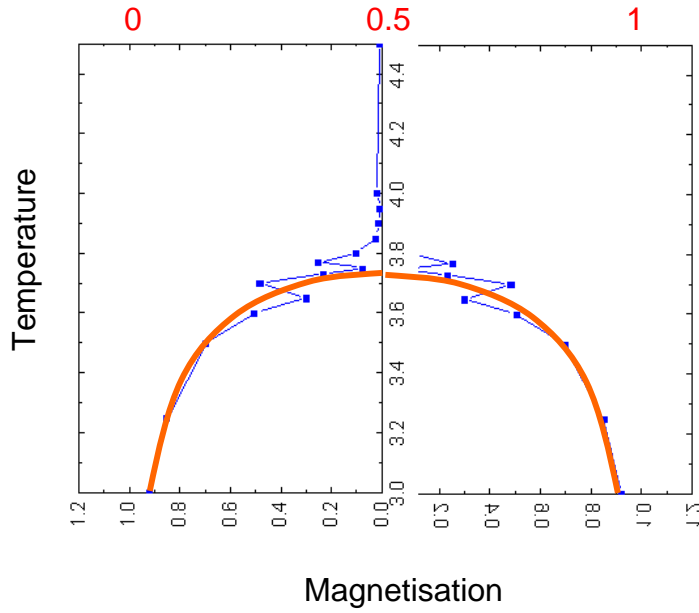


**Fig. IV.6:** Relation between the magnetisation of the Ising model (blue curve) and the coexistence curve of the lattice-gas model (red curve and red scale on the top).

Since there exists a one-to-one relation between the magnetisation of the Ising model and the coexistence curve of the lattice-gas model (see modes) are briefly discussed. Fig. IV.1) the large fluctuations near  $T_c$  in the magnetisation imply correspondingly large fluctuations in the concentration of particles in the lattice-gas model. The temperature dependence of the fluctuations are shown in Fig. IV.7.

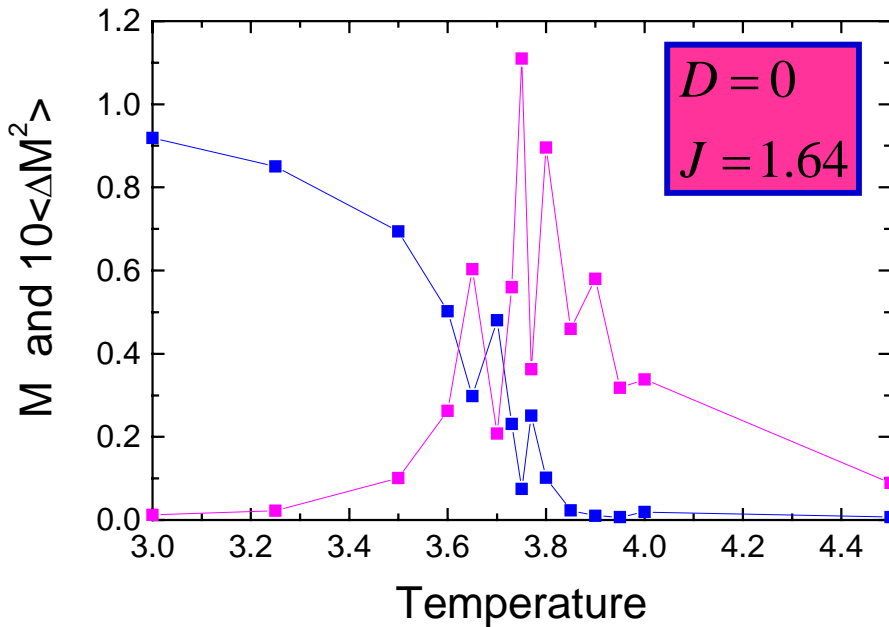


**Fig. IV.7:** Temperature dependence of the magnetisation and its mean square amplitude for an Ising model without dipolar interaction, i.e. without long range interaction. Near the critical point there is a sharp increase in fluctuations, as can also be seen in Fig. IV.5

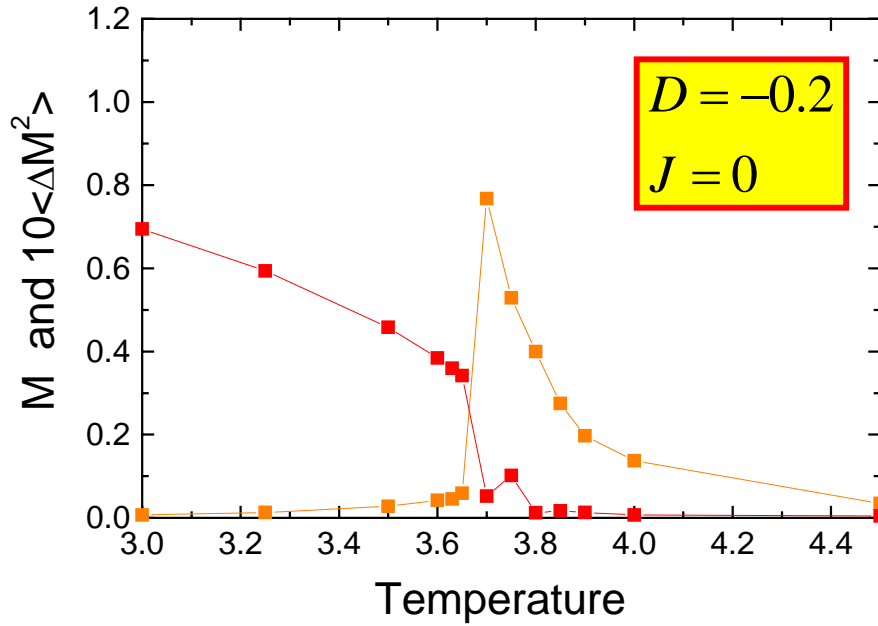


**Fig. IV.8:** Temperature dependence of the magnetisation and its mean square amplitude for an Ising model with a dipolar interaction, i.e. with a long range interaction. Since the chosen value of  $D$  is negative this case corresponds to a long range attractive interaction. Near the critical point the fluctuations are clearly reduced with respect to the case without long range interaction (see Fig. IV.7).

## IV.5 SPINODAL DECOMPOSITION

Spinodal decomposition occurs when an initially homogeneous sample at a temperature above  $T_c$  is rapidly cooled down to below the spinodal line. According to the phase diagram the system should then split into regions of dilute  $MH_x$  and regions of concentrated  $MH_x$  phases (see Fig. IV.9). As the sample cannot instantaneously change from homogeneous to fully segregated we expect that composition modulations will be set up as a function of time.

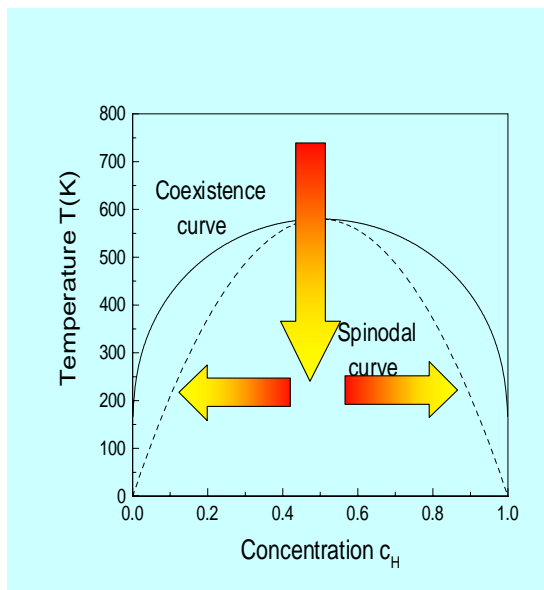


**Fig. IV.9:** Path used in the Monte-Carlo simulation to study coarsening. The system is cooled down rapidly from a temperature far above the critical point to a well below  $T_c$ . The evolution of the system is then monitored as a function of time.

This can be demonstrated with Monte-Carlo simulations. In Fig. IV.10 we show snapshots of the spin-distribution during a quench from infinite temperature down to a temperature  $T=2$  when there is only nearest-neighbour interaction, with  $J=1.64$  and  $D=0$ . The mean field critical temperature is  $T_{c\text{ mf}}= 6.56$  and the real  $T_c=0.567 \times 6.56=3.72$ . The quench temperature  $T=2$  is thus well below the critical temperature. Already after one Monte-Carlo step a clear coarsening is clearly visible.

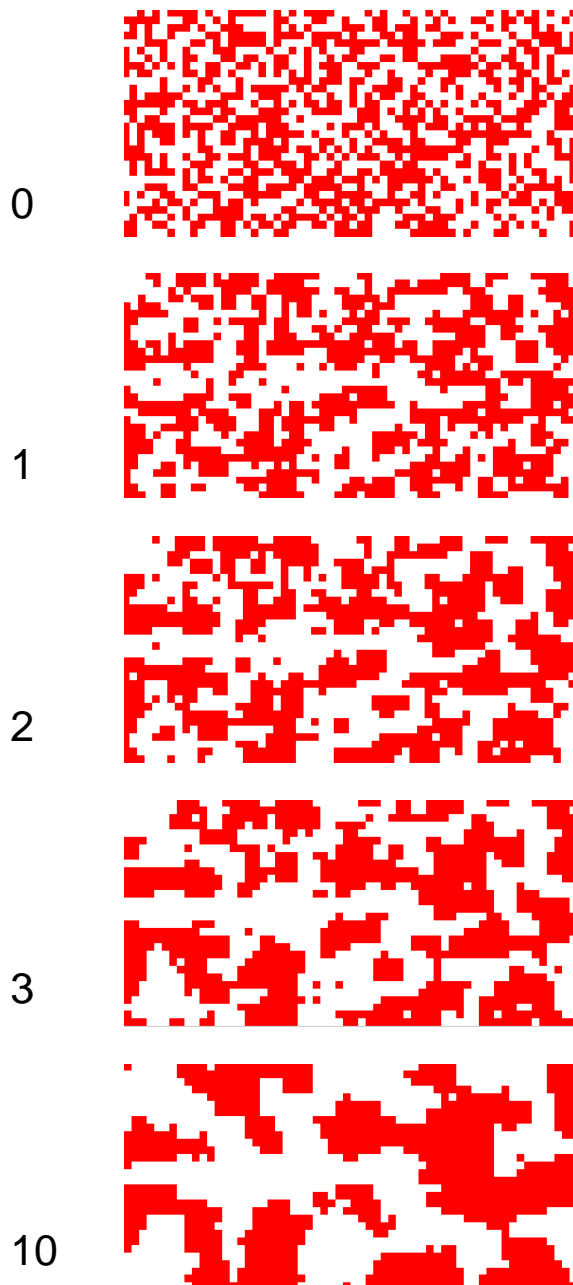


**Fig. IV.10:** Snapshots of the phase segregation occurring in a system after quenching from a random distribution corresponding to an infinite temperature (top panel) to a temperature  $T=2$  for an Ising model with only nearest-neighbour interaction. The parameter  $J=1.64$  and the corresponding critical temperature  $T_c=3.72$ . The numbers on the left indicate the Monte-Carlo step.

In Fig. IV.11 we show the results obtained for an Ising model with an attractive long range interaction corresponding to the second term in Eq.IV.80. This long range attractive interaction is also able to lead to a coarsening of the system. The obtained patterns are however clearly different from that in Fig. IV.10.

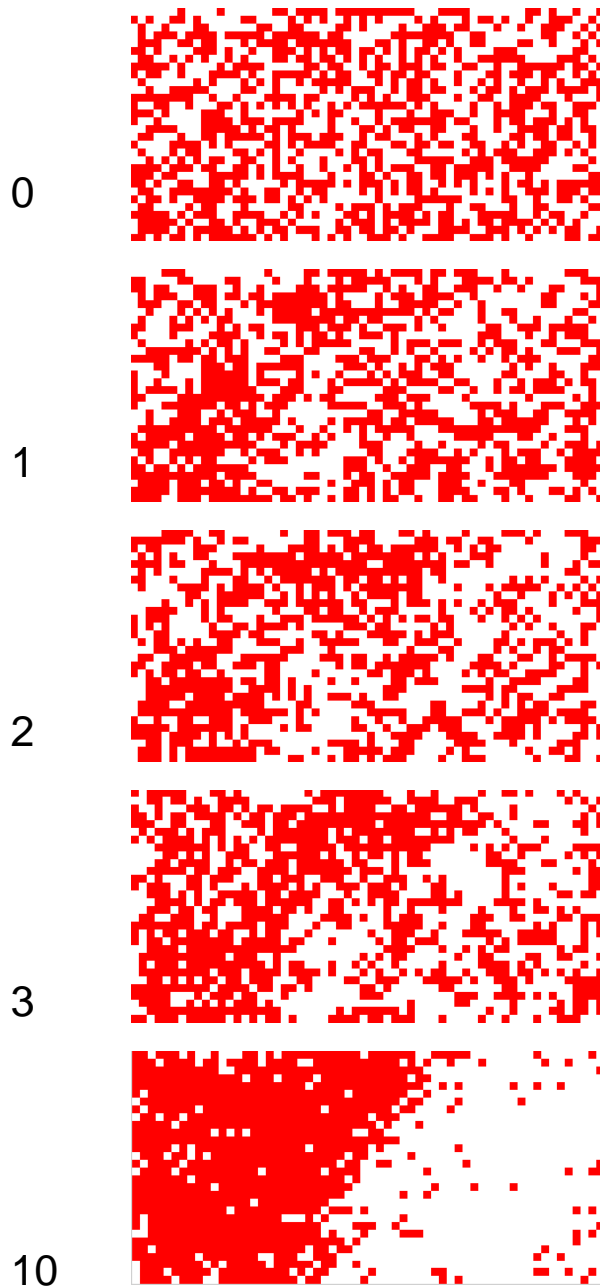


**Fig. IV.11:** Snapshots of the phase segregation occurring in a system after quenching from a random distribution corresponding to an infinite temperature (top panel) to a temperature  $T=2$  for an Ising model with only long range interaction. The parameters are  $J=0$  and  $D=-0.2$ . The corresponding critical temperature is again  $T_c=3.72$ . The numbers on the left indicate the Monte-Carlo step.

We give now a simple treatment ( Cahn<sup>9, 10, 11</sup> ) of spinodal decomposition in which it is assumed that the Gibbs free energy of the total sample is given by

$$G = \int dx \left( g(c_H) + g_{elastic}(c_H) + \alpha \left( \frac{dc_H}{dx} \right)^2 \right) \quad (IV.81)$$

where

$$g(c_H) = \frac{kTN}{V} [c_H \ln c_H + (1-c_H) \ln(1-c_H)] + N[\varepsilon_o c_H + \varepsilon \frac{n}{2} c_H^2] \quad (IV.82)$$

is the Gibbs free energy of a homogeneous phase as calculated in Eq.III.50 but expressed per unit volume. The two other terms are related to inhomogeneities in the sample. The elastic term takes into account that if the lattice remains coherent (no cracks) stresses will be generated. The energy increase associated with such stresses is

$$g_{elastic}(c_H) = \frac{E}{1-\nu} \left( \frac{d \ln a}{dc} \right)^2 (c_H - c_{H0})^2 = \eta (c_H - c_{H0})^2 \quad (IV.83)$$

where  $\eta$  is a positive parameter which is related to the Young modulus  $E$ , the Poisson ratio  $\nu$  and the concentration dependence of the lattice constant via  $d \ln a / dc$ . For a cubic crystal

$$E = C_{11} \left( \frac{(1-2\nu)(1+\nu)}{1-\nu} \right) \quad (IV.84)$$

and

$$\kappa = \frac{3(1-2\nu)}{E} \quad (IV.85)$$

The last term is the energy cost associated with the creation of interfaces between dilute  $MH_x$  regions and concentrated  $MH_x$  regions. The parameter  $\alpha$  is always positive. [Note that a similar term is also present in the Ginzburg-Landau<sup>12</sup> theory of type II superconductors. However, in these superconductors  $\alpha$  is negative. This leads to the creation of vortices].

The problem is now to find a hydrogen concentration modulation which minimises the total energy of the sample, i.e. under the condition

$$\int (c_H - c_{H0}) dx = 0 \quad (IV.86)$$

For this we define the new function

$$M = g(c_H) + g_{elastic}(c_H) + \alpha \left( \frac{dc_H}{dx} \right)^2 - \tilde{\mu}(c_H - c_{H0}) \quad (\text{IV.87})$$

and request that the variation vanishes

$$\delta \int dx \left( g(c_H) + g_{elastic}(c_H) + \alpha \left( \frac{dc_H}{dx} \right)^2 - \tilde{\mu}(c_H - c_{H0}) \right) = 0 \quad (\text{IV.88})$$

The Euler-Lagrange differential equation corresponding to this variational problem is

$$\frac{dM}{dc_H} - \frac{d}{dx} \frac{dM}{d\left(\frac{dc_H}{dx}\right)} = 0 \quad (\text{IV.89})$$

which leads to

$$\frac{dg}{dc_H} + 2\eta(c_H - c_{H0}) - 2\alpha \frac{d^2 c_H}{dx^2} - \tilde{\mu} = 0 \quad (\text{IV.90})$$

The Lagrange multiplier  $\mu$  plays the role of the chemical potential for hydrogen in the inhomogeneous sample.

$$\tilde{\mu} = \frac{dg}{dc_H} + 2\eta(c_H - c_{H0}) - 2\alpha \frac{d^2 c_H}{dx^2} \quad (\text{IV.91})$$

The diffusion of hydrogen atoms induced by a gradient in this chemical potential is

$$j_H = -L \frac{\partial \tilde{\mu}}{\partial x} \quad (\text{IV.92})$$

which can be re-written as a strain dependent diffusion equation

$$\frac{\partial c_H}{\partial t} = L \left[ \frac{d^2 g}{dc_H^2} \frac{\partial^2 c_H}{\partial x^2} + \frac{d^3 g}{dc_H^3} \left( \frac{\partial c_H}{\partial x} \right)^2 + 2\eta \frac{\partial^2 c_H}{\partial x^2} - 2\alpha \frac{\partial^4 c_H}{\partial x^4} \right] \quad (\text{IV.93})$$

by using the continuity equation for hydrogen,

$$\frac{\partial c_H}{\partial t} + \frac{\partial \tilde{J}_H}{\partial x} = 0 \quad (\text{IV.94})$$

We look now for a solution of this diffusion equation in the form of a one-dimensional modulation whose amplitude is allowed to vary with time. Inserting the Ansatz

$$c_H = C e^{i\frac{x}{\lambda}} e^{\Omega t} \quad (\text{IV.95})$$

into Eq.IV.93 we find that to lowest order the growth rate parameter  $\Omega$  is given by

$$\Omega = L \left[ - \left( \frac{d^2 g}{dc_H^2} + 2\eta \right) \left( \frac{1}{\lambda^2} \right) - 2\alpha \left( \frac{1}{\lambda^4} \right) \right] \quad (\text{IV.96})$$

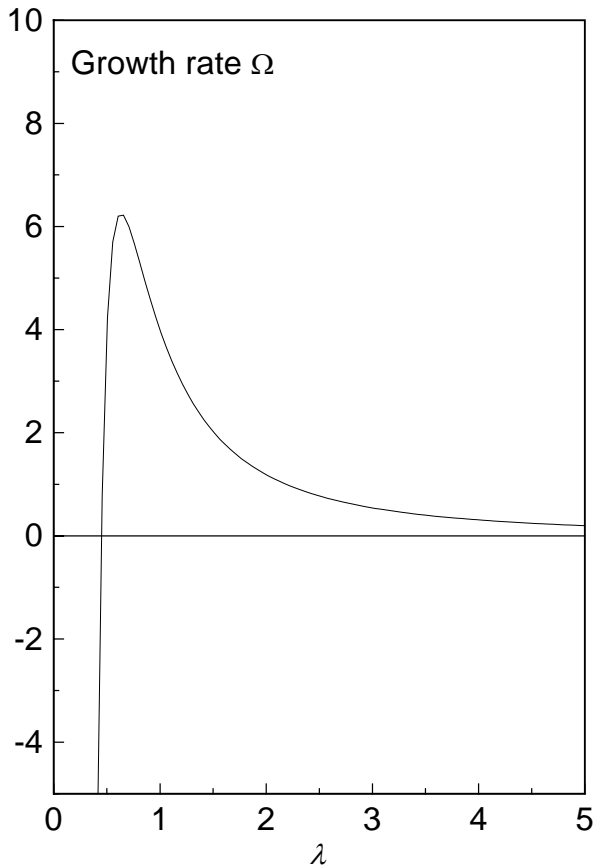


**Fig. IV.12:** Schematic representation of the dependence of the growth rate on the wavelength of the hydrogen concentration modulation. Since there is a maximum one expects that patterns with a wavelength comparable to the wavelength at the maximum will develop.

Several interesting conclusion can be drawn from this result:

- the growth rate is positive for sufficiently long wavelengths if  $\left(\frac{d^2 g}{dc_H^2} + 2\eta\right)$  is negative
- the growth rate has a maximum for  $\lambda = 2 \left(\frac{\alpha}{\frac{d^2 g}{dc_H^2} + 2\eta}\right)^{\frac{1}{2}}$
- the spinodal curve corresponding to a **coherent** situation (i.e. without dislocations) is lowered with respect to the **incoherent** one.

This last point follows directly from the definition of the spinodal region

$$\left(\frac{d\mu}{dc_H} + 2\eta\right) + 2\alpha\left(\frac{1}{\lambda^2}\right) = 0 \quad (\text{IV.97})$$

which for the lattice gas model reduces to

$$\frac{kT}{c_H(1-c_H)} + \varepsilon n + 2\eta = 0 \quad (\text{IV.98})$$

for the wave length with the largest growth rate (see b) above). This is a parabola with a maximum at  $T_{\max}$  given by

$$kT_{\max} = \frac{-\varepsilon n - 2\eta}{4} \quad (\text{IV.99})$$

This temperature is lower than  $T_c$  since  $\eta$  is positive. This implies that the coherent spinodal temperature is always lower than the incoherent one.

In the next section we will show that beside spinodal decomposition which does not depend on the shape of the sample there are also **macroscopic density modes** that depend essentially on the shape and the boundary conditions imposed to a sample.

## IV.6 THE ELASTIC H-H INTERACTION

From our analysis of various aspects of the isotherms of  $MH_x$  systems we concluded that the interaction term  $\varepsilon n$  in the lattice gas model was attractive and long ranged. At first sight the result in Eq.IV.74 does not look important, however, when one realises that the lattice spacing is typically 0.4 nm it means that the range of the H-H interaction must be much larger than 1.2 nm.

In a metal this is a large distance since electrons are very effective in screening charges. A simple estimate of the electronic screening length in metals is given by the Thomas-Fermi approximation. In this approximation the electrostatic Coulomb field produced by an ion of charge  $eZ$  embedded in a free electron gas is screened and becomes

$$V_0(r) = \frac{Ze^2 e^{-\frac{r}{r_{TF}}}}{r} \quad (\text{IV.100})$$

with

$$r_{TF} = \left( \frac{E_F}{6\pi e^2 N^*} \right)^{\frac{1}{2}} \quad \text{or in MKS-units:} \quad r_{TF} = \left( \frac{2\varepsilon_0 E_F}{3e^2 N^*} \right)^{\frac{1}{2}} \quad (\text{IV.101})$$

where  $r_{TF}$  is the so-called Thomas-Fermi screening length,  $E_F$  the Fermi energy and  $N^*$  the density of electrons. The screened potential in Eq.IV.100 decreases much faster than the unscreened  $Ze^2/r$  potential of the free ion. For a good metal such as copper, the electron density is  $8.5 \times 10^{22} \text{ cm}^{-3}$  and the Thomas-Fermi screening length is 0.055 nm. This is much shorter than the lower bound of 1.2 nm derived for the H-H interaction range from measurements near the critical point of the isotherms of  $\text{PdH}_x$ . For most metals the screening length is of the order of 0.1 nm since  $r_{TF}$  depends on the electron density only weakly through a square root function. Even for yttrium, a metal with a relatively low free electron density,  $N^* \approx 3 \times 10^{22} \text{ cm}^{-3}$ , the screening length is still short,  $r_{TF} \approx 0.08 \text{ nm}$ .

From these considerations one may safely conclude that the long-ranged H-H interaction cannot be of electronic origin. There is, however, another possibility: **an elastic interaction**. The idea is as follows: when a hydrogen atom is dissolved in a metal it induces a lattice distortion. In  $\text{PdH}_x$  the relative change in volume is about 19 % when  $x$  increases from 0 to 1. This volume change is due to a local distortion of the crystal lattice and a infinite ranged strain field. This implies that everywhere in the sample the lattice is also dilated, and consequently, more favourable for additional hydrogen atoms. To get some insight in this problem we consider the simple situation of a spherical sample of radius  $R$  in which a dilation centre has been created at its origin. The strength of this dilatation centre is the so-called dipole force tensor, which our simple case reduces to a  $3 \times 3$  diagonal matrix with elements  $P$ . One finds that the relative volume increase of the sphere is

$$\left. \frac{\Delta V}{V} \right|_{total} = 3 \frac{\Delta R}{R} = \frac{P}{V} \kappa \quad (\text{IV.102})$$

while the local lattice dilation produced by the insertion of the dilation centre at chosen place in the matrix is

$$\left. \frac{\Delta V}{V} \right|_{matrix} = \frac{P}{V} \left( \kappa - \frac{1}{C_{11}} \right) \quad (\text{IV.103})$$

where  $\kappa$  is the isothermal compressibility,  $V$  the volume of the sphere and  $C_{11}$  one of the elastic compliances which relate strains  $\varepsilon_j$  to stresses  $\sigma_i$  through

$$\sigma_i = \sum_j C_{ij} \varepsilon_j \quad (\text{IV.104})$$

from which follows directly that the compressibility can be written as

$$\kappa = \frac{3}{C_{11} + 2C_{12}} \quad (\text{IV.105})$$

and the Poisson ratio  $\nu$  (which is defined as the ratio of perpendicular strain divided by longitudinal strain in an uniaxial deformation) as

$$\nu = \frac{C_{12}}{C_{11} + C_{12}} \quad (\text{IV.106})$$

The result given in Eq.IV.102 is interesting in many respects:

- For an infinitely large sphere the local dilation of the matrix vanishes identically
- For a finite sphere made of an incompressible material, i.e. a material with a Poisson ratio equal to 1/2 the expression between brackets vanishes identically since then  $C_{11}=C_{12}$
- In any case the local dilation does not depend on the position chosen for the volume element in the sphere.

The last point is especially important for energy considerations. Assume that we add another dilation centre in the sphere. Then it will interact with the strain field set up by the first dilation centre. Its energy will be lowered by an amount

$$\Delta \varepsilon_0 = -\frac{P^2}{V} \left( \kappa - \frac{1}{C_{11}} \right) \quad (\text{IV.107})$$

which is always negative since  $\kappa - 1/C_{11}$  is always positive. In this way we find that two hydrogen atoms in an elastic medium attract each other independently of the distance which separate them. The conclusions drawn from the simple situation considered here have been shown by Wagner and Horner to hold qualitatively in a general case. In particular, Eqs.IV.102,103 and 107 can also be used to demonstrate that the boundary conditions have a very large effect on the magnitude and sign of the H-H interaction. To understand this point let us consider the problem of a sphere clamped so rigidly that the insertion of an hydrogen atom at its centre cannot modify its total volume (see Fig. IV.13). Since the dilation centre expands locally the material at the centre of the sphere the surrounding matrix must shrink, i.e.

$$\left. \frac{\Delta V}{V} \right|_{matrix} = -\frac{P}{V} \frac{1}{C_{11}} \quad (\text{IV.108})$$

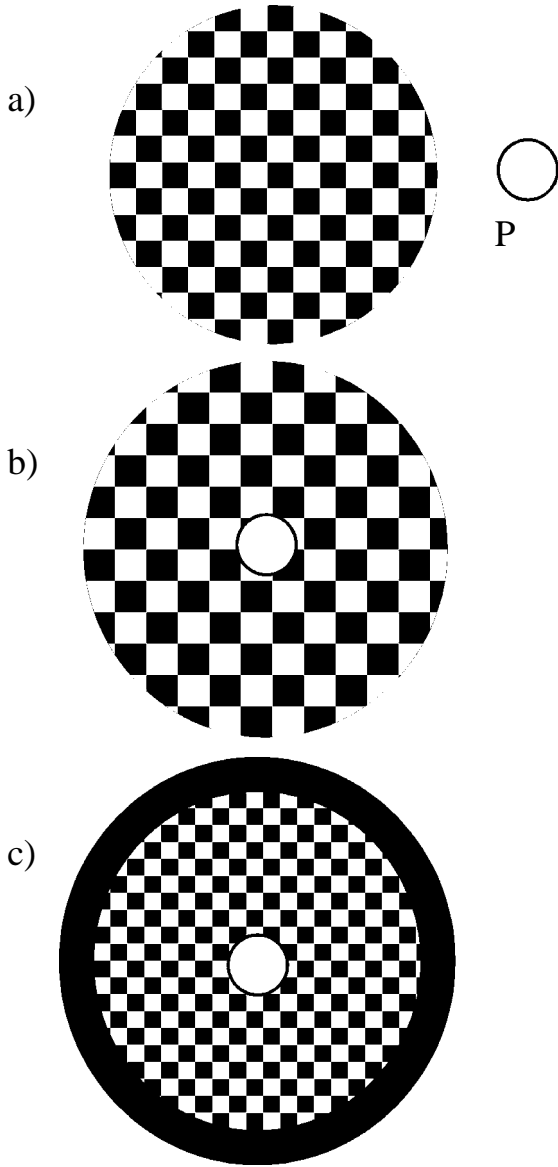


**Fig. IV.13:** Illustration of the effect of boundary conditions on the H-H interaction in a sphere<sup>13</sup>. The tile pattern symbolises the lattice of the matrix material in the undistorted case (a). When the dilation centre is introduced into a sphere of finite size with a free boundary both the total volume of the sphere and of the lattice of the matrix increase by  $\Delta V_{\text{total}}$  and  $\Delta V_{\text{matrix}}$ , respectively (see b)). In the case where the sphere is rigidly clamped at its boundary (dark ring in c)), the dilation centre causes a compression of the matrix and consequently  $\Delta V_{\text{matrix}}$  is negative. In this case the H-H interaction is repulsive while it is attractive in case b).

and the H-H interaction energy is now positive

$$\Delta \varepsilon_0 = \frac{P^2}{V} \frac{1}{C_{11}} \quad (\text{IV.109})$$

We arrive thus at the remarkable conclusion that two hydrogen atoms feel an **attractive interaction in a finite system with free surfaces** while they feel a **repulsive interaction in a perfectly clamped sample** !

Since the H-H interaction is strongly influenced by boundary conditions one can expect that the thermodynamics of  $\text{MH}_x$  systems will depend on the shape of the samples. This is beautifully shown by Zabel and Peisl<sup>14</sup> in niobium samples of various shapes. In order to prove the validity of the elastic H-H interaction model they loaded samples of niobium with hydrogen at a

concentration close to the critical concentration ( $c_c=0.31$ ) at a temperature clearly above that of the critical point ( $T_c=444$  K). Then, after a quench to below the critical temperature they followed the separation into two phases as a function of time by means of X-ray scattering. In this way they discovered that **macroscopic hydrogen density modes** were set up in the samples. In Fig. IV.14 we give an impression of these modes as a function of the sample shape.

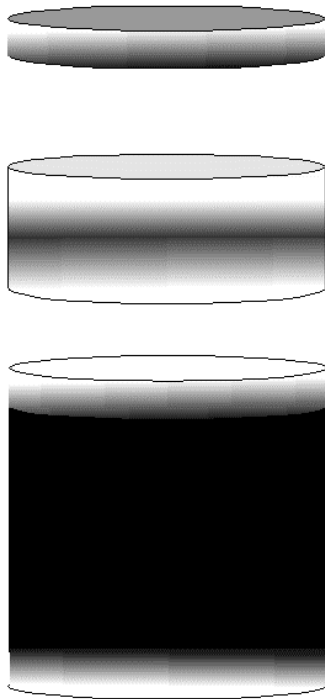


**Fig. IV.14:** Sample shape dependence of macroscopic hydrogen density modes according to Zabel and Peisl. In a disc with thickness  $L$  to diameter  $D$  ratio  $D/L=40$  the lower face contains more hydrogen than the top face and the disk deforms spherically. When the ratio is 20 there is a symmetric situation. The hydrogen-rich layer in the equatorial plane generates so much stresses that the disc splits into two halves, each being then comparable to the situation in the  $D/L=40$  sample. In a thick cylinder with  $D/L=1$  the top and bottom regions behave as in the thin samples but the central part contains probably more complex density modes.

## IV.7 LOWERING OF $T_c$ IN THIN FILMS

In thin films the clamping due to the substrate can weaken the attractive H-H interaction. This represents a case intermediate between a sample with free boundaries and a sample with fully constrained boundaries in which the H-H interaction is positive (see Fig. IV.13). Feenstra et al.<sup>15</sup> found that the critical temperature of a 122 nm thick  $\text{PdH}_x$  film is 460 K compared to 565 K in bulk  $\text{PdH}_x$  and that the critical pressure is only 3 bar compared to 20 bar in bulk. As shown in there is also a clear narrowing of the plateau region in the film.

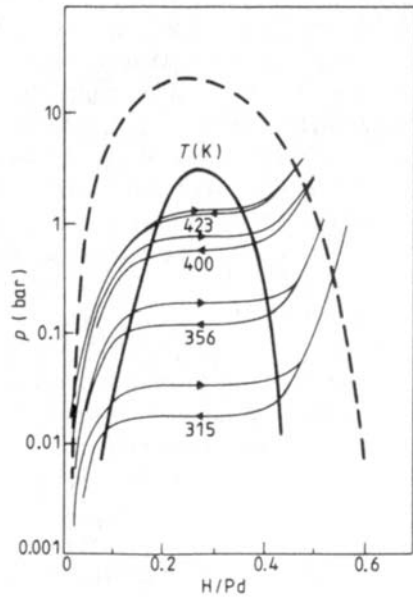


**Fig. IV.15:** The  $\alpha$ - $\beta$  coexistence curve of a 122 nm thick  $\text{PdH}_x$  film (full line) and bulk  $\text{PdH}_x$  (dashed line)

## IV.8 LOWERING OF $T_C$ IN AMORPHOUS MATERIALS

Amorphous materials can also absorb large amounts of hydrogen at moderate pressures. However, the pressure-composition isotherms of hydrogen in amorphous materials do not exhibit plateaus. This is a striking result as for some of the amorphous hydrogen absorbing materials it is known that their crystalline counterpart do exhibit plateaux. A nice example is shown in Fig for the case of  $\text{Ni}_{50}\text{Zr}_{50}$ . At 374 K the isotherm measured by Libowitz et al on crystalline  $\text{Ni}_{50}\text{Zr}_{50}$  has clearly a plateau while the isotherms of the amorphous substance are very steep. This behaviour can easily be understood in terms of a model that incorporates both disorder and H-H interaction.

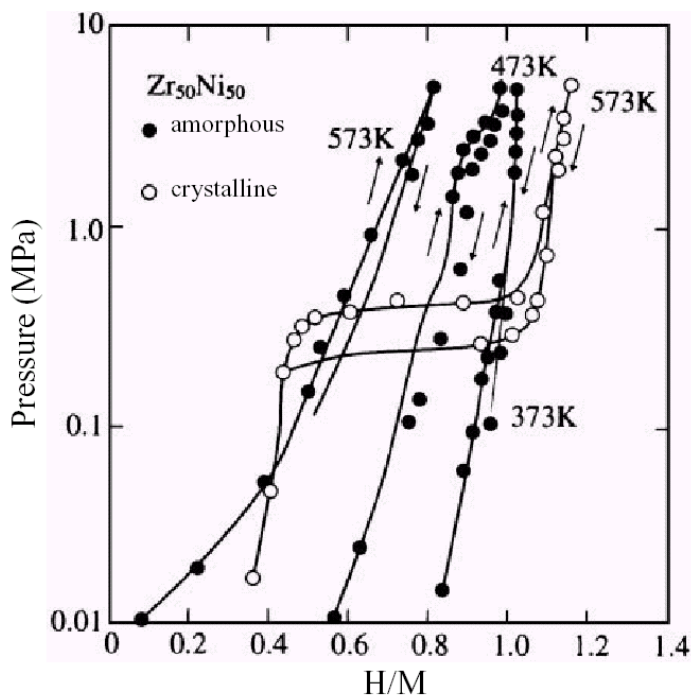


**Fig.IV.16:** Pressure-composition isotherms for H in crystalline (full line) and amorphous (dashed line)  $\text{Ni}_{50}\text{Zr}_{50}$  (from Libowitz<sup>16</sup>)

As a consequence of configurational disorder in an amorphous substance the energy  $\varepsilon$  of hydrogen at interstitial sites that can be occupied varies from site to site. The probability to find a site with energy  $\varepsilon$  between  $\varepsilon$  and  $\varepsilon+d\varepsilon$  is given by  $g(\varepsilon)d\varepsilon$ , where  $g(\varepsilon)$  is the **density of sites** function of the amorphous material under consideration.

By definition

$$\int_{-\infty}^{\infty} g(\varepsilon) d\varepsilon = 1 \quad (\text{IV.110})$$

which implies that there is on average one interstitial site per host metal atom. The concentration  $c$  of hydrogen in the alloy is then given by the implicit relation

$$\int_{-\infty}^{\infty} g(\varepsilon) x(\varepsilon, \mu_H, T, c) d\varepsilon = c \quad (\text{IV.111})$$

where  $x(\varepsilon, \mu_H, T, c)$  is the partial concentration of hydrogen occupying sites of energy  $\varepsilon$  at temperature  $T$  when the sample is in contact with hydrogen gas with a chemical potential  $\mu_{H_2}$  so that  $\mu_H = \frac{1}{2} \mu_{H_2}$ . This is the continuum limit of the situation encountered for crystalline alloys with a finite number of types of interstitial sites (see Section III.4). The distribution function  $x$  is taken as

$$c_H = \frac{1}{e^{\frac{\varepsilon_0 + f(c, T) - \mu_H}{kT}} + 1} \quad (\text{IV.112})$$

where the H-H interaction term depends on the **total** concentration of hydrogen in the sample. This is reasonable since the H-H interaction has an infinite range and depends to first order not on the exact value of the site energy. For simplicity, we assume now that  $f(c, T)$  is temperature independent and depends linearly on concentration,

$$f(c, T) = ac \quad (\text{IV.113})$$

Then Eq.IV.112 becomes

$$\int_{-\infty}^{\infty} g(\varepsilon) \frac{1}{e^{\frac{\varepsilon_0 + ac - \mu_H}{kT}} + 1} d\varepsilon = c \quad (\text{IV.114})$$

The two conditions defining the critical point (see Eq.IV.1) lead then to the following implicit relations,

$$T_c = -\frac{a}{2k} \int_{-\infty}^{\infty} g(\varepsilon) \frac{1}{\cosh z_c + 1} d\varepsilon \quad (\text{IV.115})$$

and

$$0 = \int_{-\infty}^{\infty} g(\varepsilon) \frac{\sinh z_c}{(\cosh z_c + 1)^2} d\varepsilon \quad (\text{IV.116})$$

with

$$z_c = \frac{(\varepsilon + ac - \mu_H)}{kT_c} \quad (\text{IV.117})$$

For a distribution of sites function, which is symmetric with respect to a certain energy  $\varepsilon_m$ , the integral in Eq.IV.116 can only vanish if

$$\varepsilon_m + ac - \mu_H = 0 \quad (\text{IV.118})$$

Inserting this into Eq.IV.115 gives

$$T_c = -\frac{a}{2k} \int_{-\infty}^{\infty} g(\varepsilon) \frac{1}{\cosh\left(\frac{(\varepsilon - \varepsilon_m)}{kT_c}\right) + 1} d\varepsilon \quad (\text{IV.119})$$

This relation leads immediately to the following implications:

1. The critical temperature of a disordered or amorphous system is always smaller than that of a crystalline system with the same H-H interaction. This is a direct consequence of the fact that the cosh-function is always larger than 1, so that

$$T_{c,amorphous} \leq T_{c,crystalline} = -\frac{a}{4k} \quad (\text{IV.120})$$

2. In the limit of small  $T_c$  the cosh-containing term tends towards a  $\delta$ -function. We conclude that a positive  $T_c$  is only possible when

$$-ag(\varepsilon) \geq 1 \quad (\text{IV.121})$$

This condition is analogous to the Stoner criterion for the occurrence of ferromagnetism. The attractive H-H interaction parameter for hydrogen in a metal corresponds to the exchange interaction parameter  $I$  in the Stoner theory of band ferromagnetism.

3. For a simple square-shaped density of sites function, which is zero everywhere except between  $-\Delta$  and  $\Delta$  where it equals  $1/2\Delta$  (in order to be normalized) we have

$$T_c = \frac{a}{2k} \frac{1}{2\Delta} \int_{-\Delta}^{\Delta} \frac{1}{\cosh\left(\frac{\varepsilon}{kT_c}\right) + 1} d\varepsilon \quad (\text{IV.122})$$

which implies that

$$kT_c = \frac{1}{2} \frac{y}{\ln\left(\frac{1+y}{1-y}\right)} \quad (\text{IV.123})$$

with  $y = \frac{2\Delta}{a}$ .

As expected from point 2, the critical temperature vanishes when  $ag(\varepsilon_m) = 1$  since in our case  $\varepsilon_m = 0$  and  $g(\varepsilon_m) = 1/2\Delta$ .

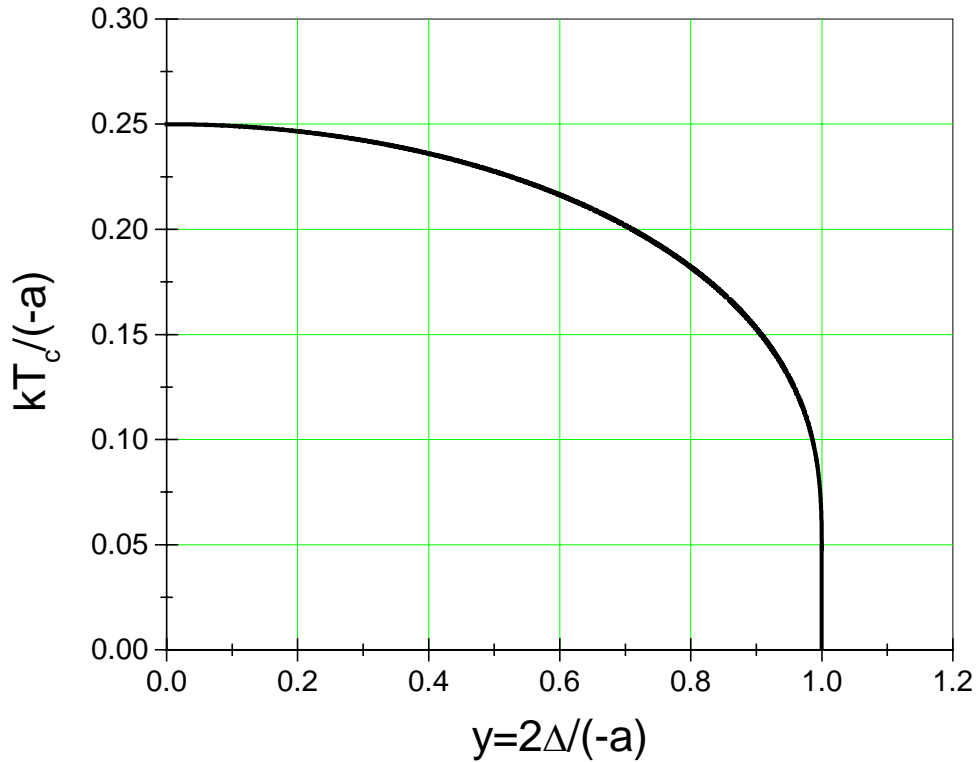


**Fig. IV.17:** Critical temperature of a disordered metal-hydride system characterised by a square-shaped distribution of sites function of width  $2\Delta$ . The strength of the attractive H-H interaction is  $a$ . In the limit  $y \rightarrow 0$ , i.e. when the distribution function tends towards a  $\delta$ -function,  $T_c \rightarrow -\frac{a}{4k_B}$ , which is the result for a crystalline solid (see Eq.III.76).

We end this Chapter by mentioning that the idea of density of sites function has been extensively used by Kirchheim and co-workers for the description in a wide class of materials and materials with specific defects. Some relevant examples are given in Fig. IV.18.

material	structure	potential trace	energy distribution	energy distribution $n(E)dE=$
single crystal				$\delta(E - E^o)$
single crystal + vacancy (or multi layer)				$(1 - c_t)\delta(E - E^o) + c_t\delta(E - E_t)$
single crystal + dislocation				$\frac{K^2}{(E - E^o)^3}$
single crystal + grain boundary				$(1 - c_t)\delta(E - E^o) + \frac{c_t}{\sigma\sqrt{\pi}} \exp\left[-\frac{(E - E_t)^2}{\sigma^2}\right]$
amorphous state				$\frac{1}{\sigma\sqrt{\pi}} \exp\left[-\frac{(E - E^o)^2}{\sigma^2}\right]$

**Fig. IV.18:** Distribution of sites function for various types of materials (Kirchheim<sup>17</sup>). The  $n(E)$  in the figure is the same as our  $g(\epsilon)$ .

## IV.9 REFERENCES

---

- <sup>1</sup> De Ribaupierre, Y., and F. D. Manchester, *J. Phys. C: Solid state Physics* **7** (1974) 2126 and 2140; de Ribaupierre, Y., and F. D. Manchester, *J. Phys. C: Solid state Physics* **8** (1974) 1339
- <sup>2</sup> De Ribaupierre, Y., and F. D. Manchester, *J. Phys. C: Solid state Physics* **6** (1973) L390
- <sup>3</sup> H. Buck and G. Alefeld, *Phys. stat. sol. (b)* **49** (1972) 317
- <sup>4</sup> Ashcroft and Mermin, *Introduction to Solid State Physics*
- <sup>5</sup> Lee, T.D., and C. N. Yang, *Phys. Rev.* **87** (1952) 404 and 410
- <sup>6</sup> Capocaccia D., and M. Vicentini-Missoni, *Rivista de Nuovo Cimento* **1**(1971)519
- <sup>7</sup> Stanley, H.E., *Introduction to Phase transitions and critical phenomena*, Univ. Press, Oxford 1971
- <sup>8</sup> L. Onsager (1944) (see Landau-Lifschitz: *Statistical Physics*, page 322)
- <sup>9</sup> Cahn, J.W., *Acta Met.* **9** (1961) 795
- <sup>10</sup> Cahn, J.W., *Acta Met.* **10** (1962) 179; **10** (1962) 907
- <sup>11</sup> Cahn, J.W., *Trans. Metall. Soc. AIME* **242** (1968) 166
- <sup>12</sup> M. Tinkham, *Introduction to superconductivity*, 2<sup>nd</sup> edition, McGraw-Hill (1996) (ISBN 0-07-064878-6)
- <sup>13</sup> D. Eshelby, *J. Appl. Phys.* **25** (1954) 255
- <sup>14</sup> Zabel, H. and H. Peisl, *Phys. Rev. Lett.* **42** (1979) 511
- <sup>15</sup> R. Feenstra, *J. Phys. F: Metal Physics* **15** (1983) L13
- <sup>16</sup> G.G. Libowitz, H.F. Hayes, and T.R.P. Gibb Jr., *J. Phys. Chem.* **62** (1958) 76; see also F.H.M. Spit, J.W. Drijver and S. Radelaar, *Scr. Metall.* **14** (1980), 1071
- <sup>17</sup> R. Kirchheim, private communication (2002)